ELSEVIER

Contents lists available at ScienceDirect

Electric Power Systems Research

journal homepage: www.elsevier.com/locate/epsr





Characterization of the initial stage in upward lightning at the Gaisberg Tower: 2. Electric field signatures

Naomi Watanabe ^{a,c,*}, Amitabh Nag ^{a,d,*}, Gerhard Diendorfer ^b, Hannes Pichler ^b, Wolfgang Schulz ^b, Hamid K. Rassoul ^a

- a Department of Aerospace, Physics and Space Sciences, Florida Institute of Technology, Melbourne, Florida, United States of America
- ^b Austrian Lightning Detection and Information System, OVE Service GmbH, Vienna, Austria
- ^c Now at the Department of Chemistry and Physics, Gulf Coast University, Fort Myers, Florida, United States of America
- ^d Los Alamos National Laboratory, Los Alamos, New Mexico, United States of America

ARTICLE INFO

Keywords: Lightning Upward lightning Initial stage Electric field measurements Electric field signatures Gaisberg Tower

ABSTRACT

We examined the characteristics of electric field signatures occurring during the initial stage of 58 flashes measured simultaneously at near (170 m) and far (79 or 109 km) distances from the Gaisberg Tower located near Salzburg, Austria. Of the 340 field signatures measured at the near station, 68 (20%) were associated with current pulses occurring during the initiation and propagation phase (IPP) of the upward leader, and 272 (80%) were associated with pulses that occurred during the mature phase (MP) of the upward leader. Of the 68 field signatures of IPP pulses, 40 were associated with bipolar (IPP-B type) current pulses and 28 were associated with unipolar (IPP-U type) current pulses. Field signatures of IPP-B pulses were only detected at the near measurement station and appear to be associated with currents in relatively short (meter-scale) channel segments formed during the upward leader inception. At the far stations, field signatures of 84 IS pulses were recorded and analyzed. There was modest correlation between the background-to-peak current of IS pulses and near and far electric radiation field changes as well as between radiation field changes recorded at near and far distances.

1. Introduction

Measurements of electric field changes at different distances from lightning processes are of fundamental interest for understanding the mechanisms as well as the modeling of such processes. Electric field signatures occurring during the initial stage (IS) of upward and rocket triggered lightning flashes measured at distances ranging from a few meters to over 100 km have been examined in various studies (e.g., [1,3, 7, 12,13]). Willett et al. [12] presented electric field signatures measured at tens of meters from the lightning channel for precursor pulses in rocket-triggered lightning in Florida. Zhou et al. [13] analyzed electric field changes measured at 170 m for M-component type and leader/RS (or mixed-mode) type of IS pulses occurring in upward flashes whose currents were measured at the Gaisberg Tower. Azadifar et al. [1] examined electric field signatures of "return-stroke-type" IS pulses overlaid on the initial continuous current (ICC) for upward lightning at the Santis Tower and reported median electric field peaks normalized to 100 km of 1.5 V/m. He et al. [3], who also analyzed upward lightning data from the Santis Tower, reported observations of electric field pulses associated with "junction processes" occurring prior to IS current pulses.

In this study, we analyze the characteristics of electric field signatures occurring during the IS of 58 flashes measured simultaneously at near (170 m) and far (79 or 109 km) distances from the Gaisberg Tower between 2006 and 2014. The current pulses that occurred during the IS in these flashes are analyzed in part 1 ([9], this issue). In this part, we also examine the relationship between various parameters of current and electric field pulses.

2. Instrumentation and data

Two electric field measurement systems at the near and far distances of 170 m and 79 km (during 2006–2007) or 109 km (2008 onwards), respectively, from the Gaisberg Tower were used to measure the electric field signatures associated with upward lightning initiated from the tower. Each electric field measurement system consisted of a flat plate antenna with an active integrator and amplifier. For the measurement system at 170 m, the integrator output was sent to a 12-bit digital acquisition system via a fiber optic link (ISOBE 5000, with bandwidth

E-mail addresses: nwatanabe@fgcu.edu (N. Watanabe), anag@fit.edu (A. Nag).

^{*} Corresponding authors.

from DC to 25 MHz). For the measurement system at 79 or 109 km, a fiber optic link was used up to July 2013 after which a double shielded coaxial cable was used to transmit the data from the integrator to a 12-bit digital acquisition system. Both (near and far) field measurement systems had an overall frequency bandwidth from 300 Hz (which translates to a decay time-constant of 0.5 ms) to 1 MHz. Note that, the time-constant of 0.5 ms was insufficient to faithfully record the ten-millisecond-scale field changes due to upward leaders. So, we digitally compensated for the decay time-constant of the measurement (e.g., [4,5,8]) to obtain "corrected" electric fields. The sampling rate was 5 MHz (sampling interval of 200 ns) and the record length was 5 s, with a 2-s pre-trigger time. The electric field records were GPS time-stamped and were triggered using a trigger-signal transmitted from the current measurement station at the Gaisberg Tower.

The near field measurement system was installed on a 4-m high metal platform located on top of the Gaisberg mountain. The field enhancement factors on top of the platform (with respect to nearby flat ground) and on top of the mountain (with respect to the bottom of the

mountain) were, respectively, 7.8 and 2.8 ([14]). During 2006–2007 the far-field measuring system was installed on top of a building in Wels, Austria (a small city, 79 km from the tower). No amplitude calibration was available for the far-field measurement for data collected in this period. In our analysis, we did not use the magnitude of the electric field amplitude of pulses to draw any conclusions. Starting 2008, the far-field measuring system was located on the roof of a building in Neudorf, Austria (a small village, 109 km from the tower). A field enhancement factor of 2.5 was determined for the antenna location on the roof of the building with respect to nearby flat ground [2].

We examined the characteristics of 340 electric field signatures (associated with IS current pulses) occurring in 50 flashes (of the 58 in our dataset) measured at the near-field station. Also, 84 field signatures in 11 flashes that were measured at the far-field station, were analyzed.

3. Characteristics of IS electric field signatures

Fig. 1a-c show the IS current, as well as electric field waveforms

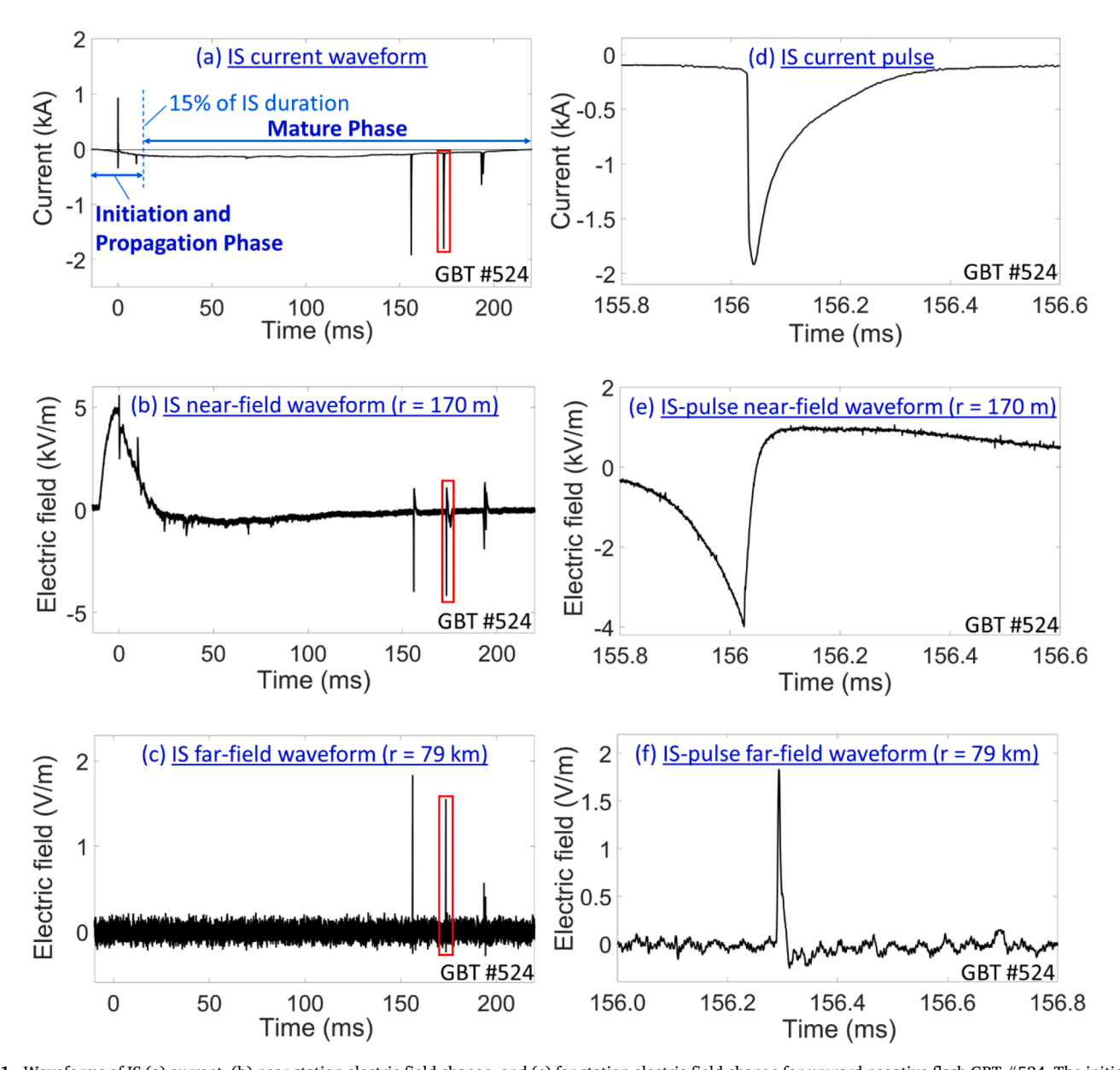


Fig. 1. Waveforms of IS (a) current, (b) near-station electric field change, and (c) far-station electric field change for upward negative flash GBT #524. The initiation and propagation phase (IPP) and mature phase (MP) for this flash are labelled in (a). The red rectangles in (a), (b), and (c) indicate a "classical" IS pulse in this upward flash whose (d) current (e) near-field, and (f) far-field waveforms are shown on an 800-µs timescale.

measured at near and far distances for a negative upward flash (GBT #524) that occurred at the Gaisberg Tower. Fig. 1d–f show a typical "classical" IS current pulse along with its near and far electric field waveforms.

We analyzed the characteristics of electric field signatures measured at the near and far stations that occurred during the initiation and propagation phase (IPP) and mature phase (MP) of the IS (see part 1, [9], this issue). Fig. 2a shows bipolar current pulses (in black) that occurred at early times (in this case, within the first 3 ms of flash-start) during the IPP (that we called IPP-B pulses in part 1, [9], this issue) and the associated electric field waveform (in blue) measured at 170 m from the Gaisberg Tower in flash GBT #473. Fig. 2b shows the definitions of the various parameters that we measured for such electric field signatures of IPP-B pulses. Note that none of our IPP-B current pulses produced a measurable far-field signature.

Figs. 3a and b show the definitions of the various parameters we measured for near- and far-field signatures, respectively, corresponding to "classical" IS current pulses that occurred during the MP. Also, typical unipolar current pulses occurring during the IPP (IPP-U pulses, see part 1, [9], this issue) produced similar field signatures (see Fig. 4). The inset in Fig. 3a shows the radiation field peak embedded in the near field signature which is dominated by the electrostatic component of electric field. The far-field signature in Fig. 3b is essentially that of the radiation component of electric field. In the following sub-sections, we present the results of our analysis of electric field waveform parameters measured at near and far distances corresponding to IPP and MP current pulses.

3.1. Electric field signatures at the near station

At the near field station at a distance of 170 m from the tower,

13 (a) 1 IPP-B current pulses Current (kA) 11 0 9 Electric field (Near field waveform (r = 170 m) -2 GBT #473 2.78 2.9 2.82 2.84 2.86 2.88 2.8 Time (ms) (b) IPP-B pulse near-field waveform (r = 170 m) Electric field (kV/m) **Total duration** 10-to-90% risetime Background field level 10% field change Full-width at half-maximum 50% 90% GBT #473 Background-to-peak risetime 2.81 2.811 2.812 2.813 2.814 2.815 Time (ms)

electric field signatures corresponding to 340 IS current pulses were measured. Of these 340 field signatures, 68 (20%) occurred during the IPP and 272 (80%) occurred during the MP. We categorized the IPP electric field signatures into two types based upon the waveshape of the corresponding current pulses; electric field signatures for bipolar and unipolar current pulses were labeled as IPP-B and IPP-U, respectively. Of the 68 IPP-pulse field signatures, 40 (59%) were of the IPP-B type and 28 (41%) of the IPP-U type. Example of IPP-B current pulses and associated near-field signature is shown in Fig. 2. Example of an IPP-U current pulse and associated near-field signature is shown in Fig. 4a and b, respectively. As can be seen from these figures, the overall near-field signatures associated with IPP-B and IPP-U pulses are distinctly different; the IPP-B field signatures consist of bipolar pulses with relatively small electrostatic field change after each pulse while the IPP-U field signatures resemble those of "classical" IS pulses occurring during the MP (see, e.g., Figs. 3a and 5b). The reason for the difference in the overall electric field signatures of IPP-B versus IPP-U and MP pulses is likely due to IPP-B current pulses being associated with inception-processes of upward leaders (see the discussion in Section 4).

Fig. 6 shows the histograms for the following electric field parameters (defined in Fig. 2b) for 40 IPP-B pulses (occurring in 18 of the 58 flashes in our dataset): background-to-peak risetime, 10–90% risetime, full-width at half-maximum (FWHM), and background-to-peak field change. The background-to-peak risetimes (Fig. 6a) ranged from 0.59 to 2.0 μs , with median being 1.0 μs . The 10–90% risetimes (Fig. 6b) ranged from 0.15 to 1.5 μs , with median being 0.69 μs . The FWHM (Fig. 6c) ranged from 0.14 to 1.4 μs , with median being 0.43 μs . The background-to-peak field changes (Fig. 6d) ranged from 0.03 to 1.7 kV/m, with median being 0.37 kV/m. After accounting for the enhancement factor of 7.8 due to the 4-m high metal platform on which the electric field

Fig. 2. (a) Upper (in black) and lower (in blue) waveforms show, respectively, the bipolar current pulses (scale shown on the left vertical axis) that occurred at early times during the IPP (that we called IPP-B pulses in part 1, [9], this issue) and the associated electric field changes (scale shown on the right vertical axis) measured at 170 m from the Gaisberg Tower in flash GBT #473. (b) Electric field signature of an IPP-B pulse measured at 170 m from the Gaisberg Tower in flash GBT #473, shown on a 50-µs time scale along with the various parameters examined in this study.

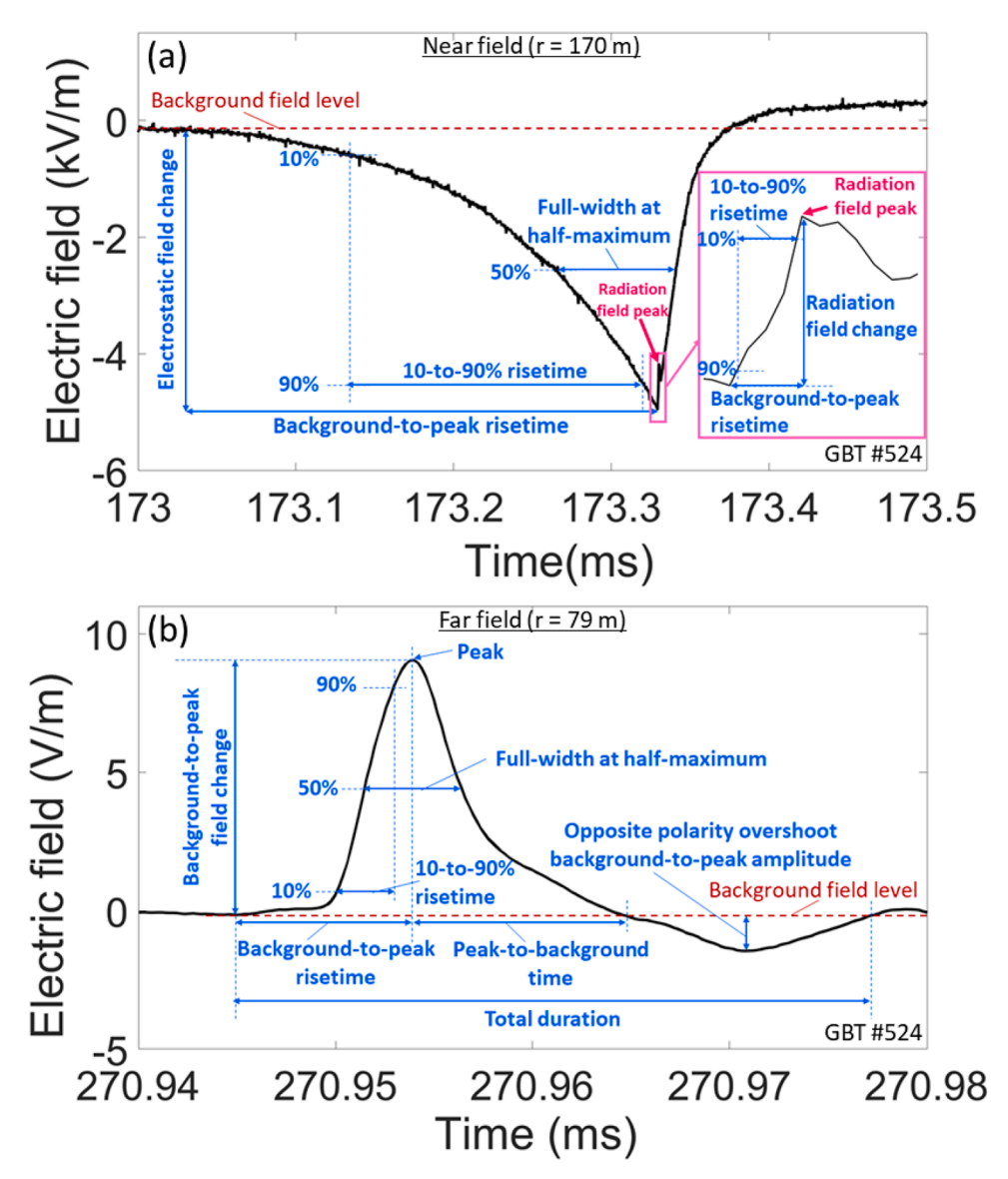


Fig. 3. Electric field change waveforms measured at (a) near and (b) far stations corresponding to two different "classical" IS current pulses that occurred during the MP in flash GBT #524. Shown are the various electric field waveform parameters examined in this study. The inset in (a) shows, in an 500 μ s timewindow, the radiation field peak embedded in the near field signature (which is dominated by the electrostatic component of electric field); the background-to-peak radiation field change was 807 V/m. The far-field signature in (b) is essentially that of the radiation component of electric field.

sensor was located, the median electric field change was 47 V/m referenced to flat ground at 170 m from the base of the tower.

Fig. 7a-d show histograms of the electric field background-to-peak risetime, 10-90% risetime, FWHM, and background-to-peak electrostatic field change color-coded in blue and pink for 28 IPP-U (occurring in 18 flashes), and 272 MP (occurring in 35 flashes) pulses, respectively; these parameters are defined in Fig. 3a. The background-to-peak risetimes (Fig. 7a) ranged from 0.8 µs to 3.1 ms, with the median being 314 $\mu s.$ For IPP-U and MP pulses, the median risetimes were 69 and 337 $\mu s,$ respectively. The 10–90% risetimes (Fig. 7b) ranged from 0.52 μs to 2.2 ms, with the median being 156 μ s. The median for IPP-U and MP pulses were 34 and 185 µs, respectively. The median background-to-peak and 10-90% risetimes were, respectively, 4.9 and 5.4 times longer for MP than those for IPP-U pulses. The FWHM (Fig. 7c) and electrostatic field change (Fig. 7d) for both IPP-U and MP pulses taken together ranged from 0.45 µs to 4.1 ms and 8.3 V/m to 19 kV/m, respectively, with the medians being 95 µs and 1.6 kV/m, respectively. After accounting for the enhancement factor of 7.8, the median electrostatic field change was 0.17 kV/m referenced to flat ground at 170 m from the base of the tower. The median FWHM was 3.5 times longer for MP (107 µs) pulses than that for IPP-U (31 µs) pulses, and the median electrostatic field change was 4.3 times higher for MP (1.8 kV/m) pulses than that for IPP-U (0.42 kV/ m) pulses.

For 10 (of 28) IPP-U and 73 (of 272) MP pulses occurring in 5 and 12 flashes, respectively, a radiation field peak was observed in the near electric field signature, as shown in Fig. 3a (see also the inset). Fig. 8 shows the histograms for background-to-peak risetime, 10-90% risetime, and background-to-peak radiation field change color-coded in blue and pink for IPP-U and MP pulses, respectively. Note that, even though we label the field change leading to the radiation field peak (see Fig. 3a) as the "radiation" field change, it likely contains some contributions from the electrostatic and induction components of electric field as well. The background-to-peak risetimes (Fig. 8a) ranged from 0.2 to 2.8 μs , with the median being 0.71 µs. For IPP-U and MP pulses, the median risetimes were 0.62 and 0.71 µs, respectively. The 10-90% risetimes (Fig. 8b) ranged from 0.11 to 1.5 μ s, with the median being 0.35 μ s. The median for IPP-U and MP pulses were 0.38 and 0.35 µs, respectively. The median background-to-peak and 10-90% risetimes were similar for IPP and MP pulses. The background-to-peak radiation field change (Fig. 8c) ranged from 0.16 to 15 kV/m, with the median being 1.7 kV/m. After accounting for the enhancement factor of 7.8, the median field change for the radiation field peak was 0.22 kV/m referenced to flat ground at 170 m from the base of the tower. The median radiation field change was 3.1 times larger for MP (1.7 kV/m) than IPP-U (0.54 kV/m) pulses.

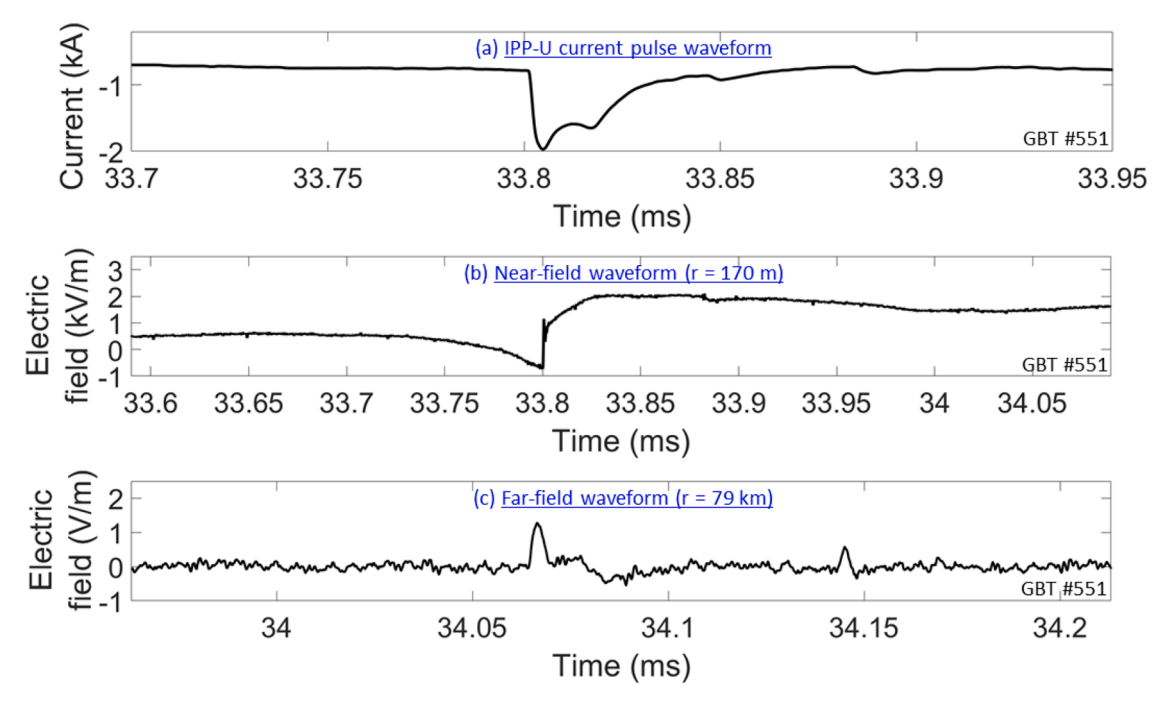


Fig. 4. (a) Current, (b) near-field, and (c) far-field waveforms for an IPP-U pulse that occurred during the IS of upward negative flash GBT #551, shown on a 250-µs time scale.

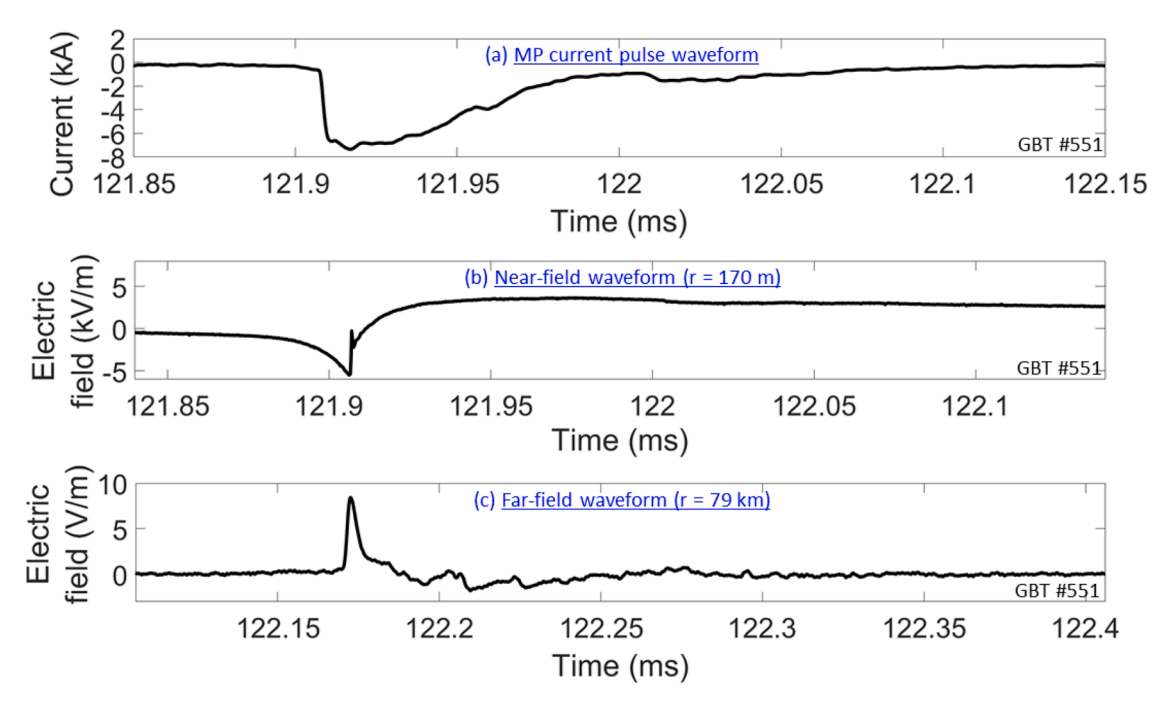


Fig. 5. a) Current, (b) near-field, and (c) far-field waveforms for an IS pulse that occurred during the MP of upward negative flash GBT #551, shown on a 300-µs time scale.

3.2. Electric field signatures at the far station

At the far field stations at distances of 79 km (Wels) and 109 km (Neudorf) from the Gaisberg Tower, the field changes were essentially due to the radiation component of electric field. Field changes associated with 89 IS current pulses were detected (with peak electric field amplitudes greater than 1.5 times the background noise level). These pulses occurred in 11 of the 58 flashes in our dataset. We included in our analysis 84 field signatures (also in 11 flashes) that had peak electric field amplitudes greater than twice the background noise level. Of these

84 field signatures, only one (in one flash) was recorded at Neudorf and the other 83 (in 10 flashes) were recorded at Wels. Also, six of the 84 IS current pulses associated with these field signatures occurred during the IPP (all six, including the one whose field signature was recorded at Neudorf, were of the IPP-U type) and 78 occurred during the MP.

Fig. 3b shows the various parameters of the electric field signatures measured at the far stations that we analyzed. Examples of far field signatures for IPP-U and MP pulses are shown in Figs. 4c and 5c, respectively. Fig. 9 shows the histograms for background-to-peak risetime, 10–90% risetime, and background-to-peak field change color-

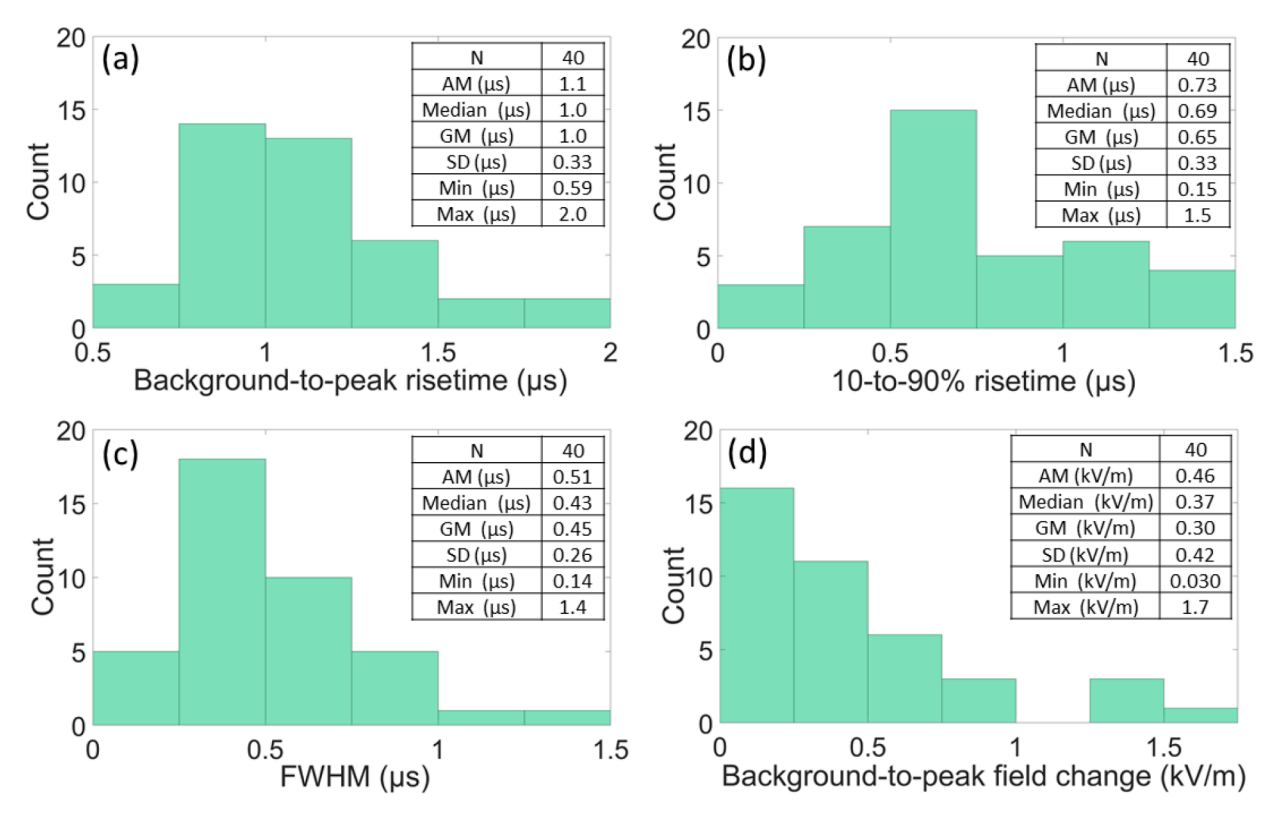


Fig. 6. Histograms showing (a) background-to-peak risetime, (b) 10-to-90% risetime, (c) FWHM, and (d) background-to-peak field change for 40 electric field signatures of IPP-B pulses, occurring in 18 of the 58 flashes in our dataset, measured at 170 m from the Gaisberg Tower. Arithmetic mean (AM), median, geometric mean (GM), standard deviation (SD), maximum (Max), and minimum (Min) values are shown in the table in each histogram. Note that, field enhancement factors on top of the platform (with respect to nearby flat ground) and on top of the mountain (with respect to the bottom of the mountain) were, respectively, 7.8 and 2.8, which can be applied to the histogram and statistics shown in (d).

coded in blue and pink for five IPP-U and 78 MP pulses, respectively. Note that we have excluded the electric field signature for one IPP-U pulse that was recorded at Neudorf from these histograms. Also, for our far field signatures the "background" refers to the zero field-level at the beginning of the electric field signatures. The background-to-peak risetimes (Fig. 9a) ranged from 1.1 to 41 µs, with the median being $2.5 \, \mu s$. For IPP-U and MP pulses, the median risetimes were $1.8 \, and \, 2.8$ μs, respectively. The 10-90% risetimes (Fig. 9b) ranged from 0.7 to 23 μs , with the median being 1.4 μs . The medians for IPP-U and MP pulses were 1 and 1.4 µs, respectively. The median background-to-peak risetime was somewhat longer for field signatures of MP than that for field signatures of IPP-U pulses, while the median 10-90% risetimes were similar. The FWHM (Fig. 9c) ranged from 1.4 to 17 μ s, with the median being 3.1 μ s. The medians for IPP-U and MP-pulse field signatures were 2.7 and $3.2~\mu s$, respectively. The background-to-peak field change (Fig. 9d) ranged from 0.9 to 12 V/m, with median being 2.5 V/m. No amplitude calibration was available for the Wels measurement station; the field enhancement factor due to the building on which the electric field sensor was installed was unknown. Therefore, these electric field changes should be treated as overestimates of those measured at ground level, perhaps by a factor of 2-3. The median background-to-peak electric field change was two times larger for MP (2.6 V/m) than IPP-U (1.3 V/m) pulses. Finally, the background-to-peak risetime, 10-90% risetime, FWHM, and background-to-peak field change for the IPP-U pulse recorded at Neudorf were 28.6 µs, 12.7 µs, 11.0 µs, and 10.3 V/ m, respectively. After accounting for the building enhancement factor of 2.5 (see Section 2), the electric field change was 4.1 V/m on flat ground at the base of the building. Fig. 10 shows the histograms for peak-tobackground time, opposite polarity overshoot background-to-peak amplitude, ratio of opposite polarity overshoot to initial peak, and total duration. The peak-to-background time (Fig. 10a) ranged from 3.5 to 35 μ s, with the median being 10 μ s. For IPP-U and MP pulses, the median times were 7.2 and 10 μ s, respectively. The opposite polarity overshoot background-to-peak amplitude (Fig. 10b) ranged from 0.02 to 3.8 V/m, with the median being 0.51 V/m. The medians for IPP-U and MP pulses were 0.61 and 0.50 V/m, respectively. The ratio of opposite polarity overshoot to initial peak (Fig. 10c) ranged from 0.01 to 0.84, with the median being 0.21. The medians for IPP-U and MP-pulse field signatures were 0.51 and 0.19, respectively. The total duration (Fig. 10d) ranged from 5.4 to 148 μ s, with the median being 32 μ s. For IPP-U and MP-pulse field signatures, the medians were 23 and 33 μ s, respectively. The peak-to-background time, opposite polarity overshoot background-to-peak amplitude, ratio of opposite polarity overshoot to initial peak, and total duration for the IPP-U pulse recorded at Neudorf were 40 μ s, 10 V/m (4 V/m on flat ground at the base of the building), 0.97, and 75 μ s, respectively.

4. Discussion

Of the 340 electric field signatures measured at the near field station, 68 occurred during the IPP of the IS (which is the early part of the IS, see part 1, [9], this issue). The majority (40 of 68 or 59%) of these electric field signatures were associated with IS current pulses of the IPP-B type. These current pulses are similar to the precursor pulses in rocket-triggered lightning reported in various studies (e.g., [10,11,12]). We hypothesize that these pulses could be associated with the formation of corona/streamers preceding the development of short leader segments at the time of upward leader inception. Generally speaking, we expect the electric field signatures associated with lightning processes that involve currents in relatively long channels to be dominated by the electrostatic component (which is proportional to the integral of current, i.e., charge) at a distance of 170 m (distance from the Gaisberg Tower to

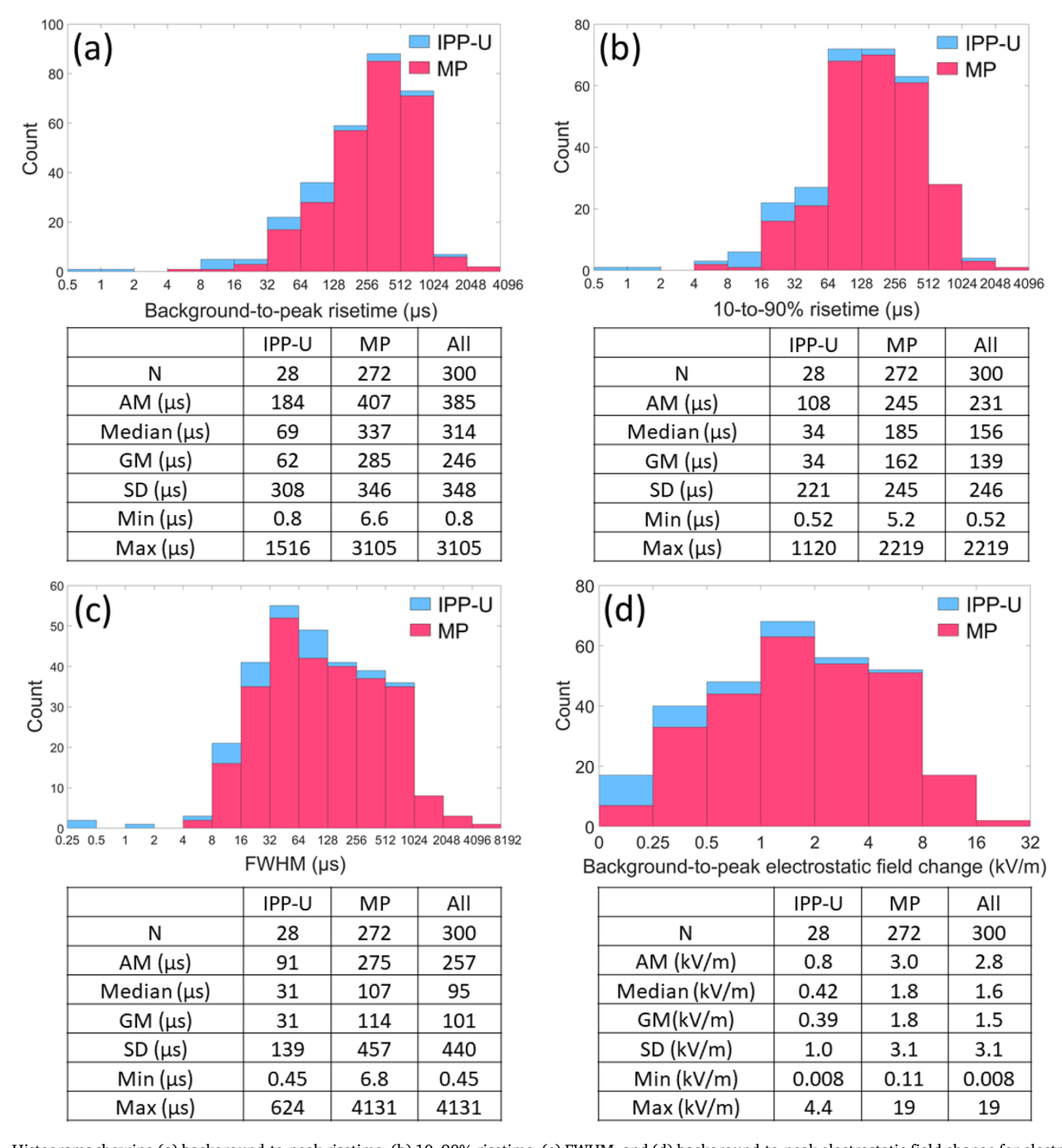


Fig. 7. Histograms showing (a) background-to-peak risetime, (b) 10–90% risetime, (c) FWHM, and (d) background-to-peak electrostatic field change for electric field signatures of 28 IPP-U and 272 MP pulses occurring in 18 and 35 flashes, respectively, measured at 170 m from the Gaisberg Tower. Statistics for IPP-U, MP, and all unipolar pulses are shown in the table below each histogram. See also caption of Fig. 6 for note on the field enhancement factors that can be applied to (d).

the near field measurement station). This is applicable for the IPP-U and MP pulses in our dataset (see e.g., Figs. 4 and 5). However, as can be seen from Fig. 2, the IPP-B electric field signatures consist of microsecond-scale bipolar pulses, with each pulse being followed by a relatively small electrostatic field change. If IPP-B pulses are indeed related to corona/streamers preceding the development of short leader segments, the electric field signatures of such current pulses will be related primarily to currents in relatively short (meter-scale) channel segments formed during the upward leader inception. If such a short channel segment is represented as a Hertzian dipole, the field change will be proportional to the derivative of the source-current (e.g., [6]). As a result, the near-station electric field signatures of these IPP-B pulses are less dominated by the electrostatic component than those of IPP-U

and MP pulses; the latter two pulse-types are likely associated with currents in relatively long (few tens of meters or longer) channels after the development of a self-sustaining upward leader. Also, no electric field change associated with these bipolar IS current pulses were detected at the far field measurement stations. This indicates that these electric field signatures were relatively low amplitude; they were associated with small amounts of charge being moved over short (perhaps less than a few meters) distances. The lack of measureable far-field signatures of IPP-B pulses supports our hypothesis that the bipolar current pulses occurring at the beginning of the IS are due to streamers preceding the development of a self-sustaining upward leader.

For 52 IS pulses (5 IPP-U and 47 MP), a radiation field peak was observed in both the near (170 m from the Gaisberg Tower) and far (79

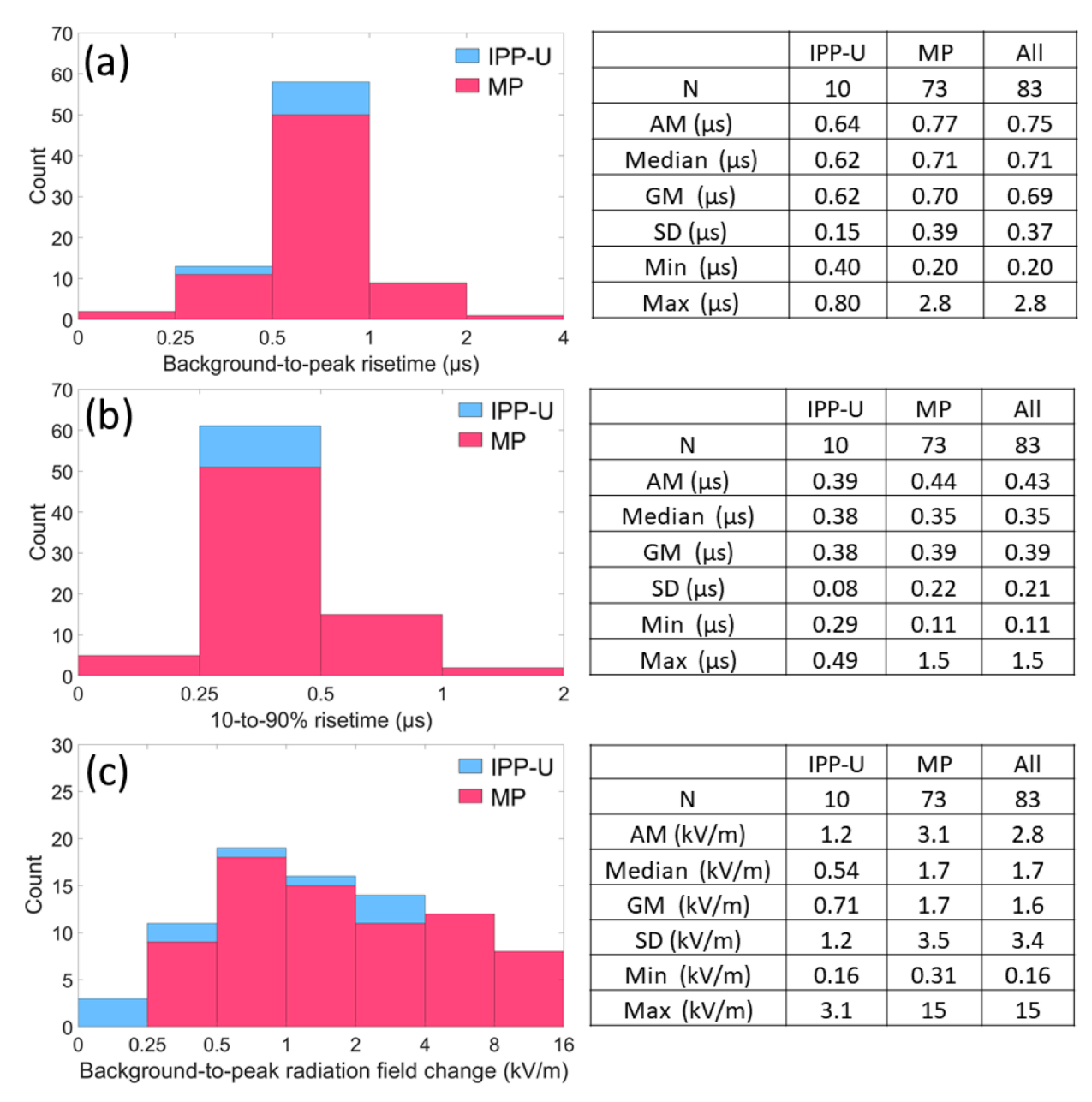


Fig. 8. Histogram of (a) background-to-peak risetime, (b) 10–90% risetime, and (c) background-to-peak radiation field change for electric field signatures of 10 IPP-U and 73 MP pulses occurring in 5 and 12 flashes, respectively, measured at 170 m from the Gaisberg Tower. Statistics for IPP-U, MP, and all unipolar pulses are shown in the table adjoining each histogram. See also caption of Fig. 6 for note on the field enhancement factors that can be applied to (c).

km from the tower) electric field signatures allowing us to compare the characteristics of the rising portion of their current and electric field waveforms. Fig. 11 shows the scatter plots of background-to-peak amplitudes and risetimes of current versus electric field as well as near-field versus far-field. The blue and pink color-coding indicates IPP-U and MP pulses, respectively. The coefficients of determination (R²) are shown in the figures. As seen in Fig. 11a and b, as the background-to-peak current amplitude increases, the radiation field change at near and far stations, respectively, tend to increase; there is modest correlation between current and field amplitudes ($R^2 = 0.48$ and 0.73, respectively). Far field amplitudes also tend to increase with increasing near (radiation) field amplitudes with modest correlation ($R^2 = 0.64$), as seen in Fig. 11c. On the other hand, as seen from Figs. 11d-i, current versus field risetimes (both background-to-peak and 10-90%) as well as near versus far-field risetimes were essentially uncorrelated with very small determination coefficients. One factor that contributes to the determination coefficient being lower between the background-to-peak amplitudes of current and radiation field change measured at the near station (see Fig. 11a) than that between amplitudes of current and far-field change is that the radiation field signatures measured at the near station are expected to be somewhat "contaminated" by induction and electrostatic components of electric field which are more dominant at short distances from relatively long current carrying channels. Such "contamination" would also affect the measured risetimes for the radiation field signature recorded at the near station. Finally, the effect of propagation over lossy soil is expected to impact the risetimes of electric field signatures at the far station. Note that, similarly low determination coefficients between current and far field FWHM for return strokes at the Gaisberg Tower was reported by Pichler et al. [7]. Also note that the aspects of electric fields mentioned above along with the effect of upward leader channel geometry (which can be significantly different from vertical) result in relatively diverse electric field signatures for IS current pulses. This diversity is noticeable

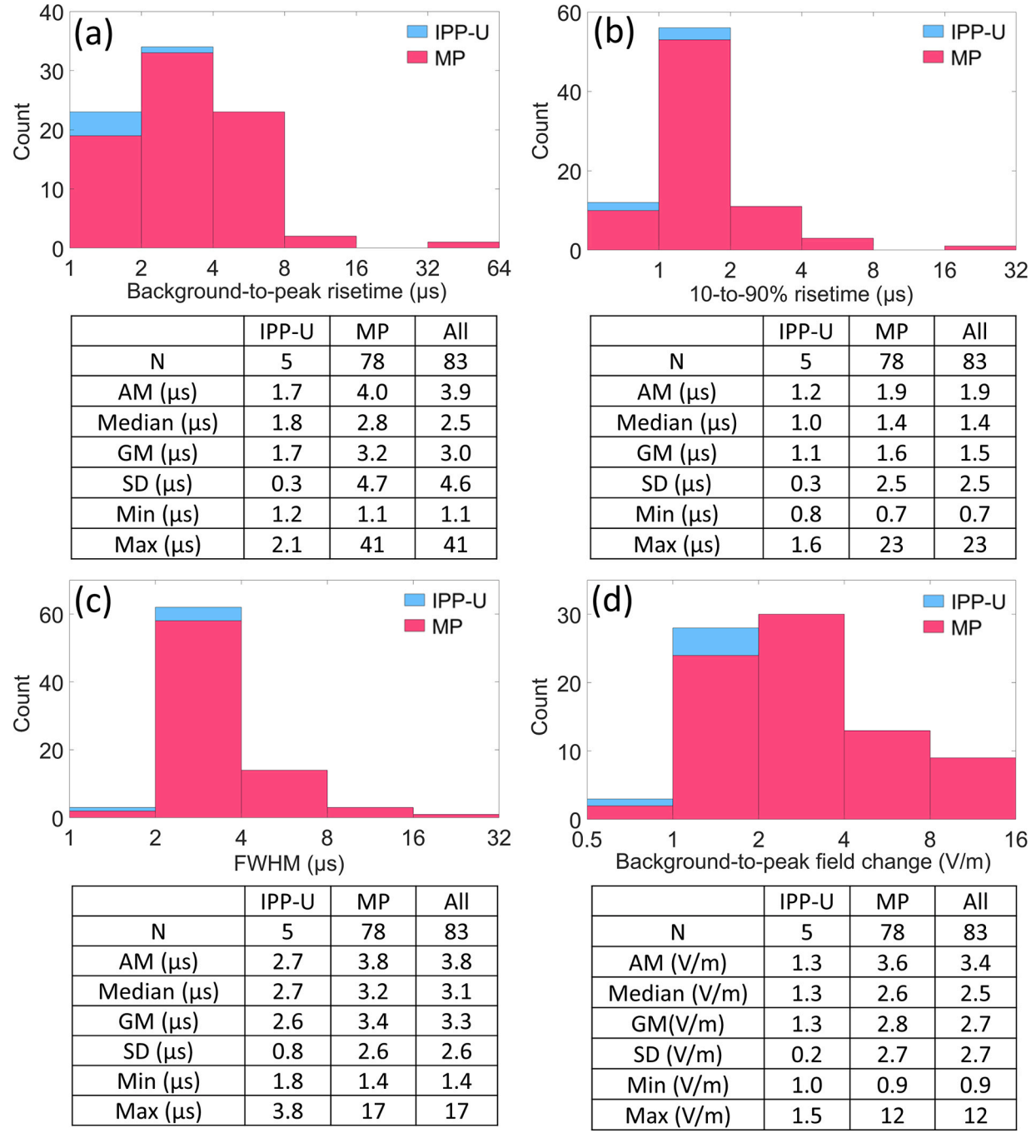


Fig. 9. Histogram of (a) background-to-peak risetime, (b) 10–90% risetime, (c) FWHM, and (d) background-to-peak field change for electric field signatures of 5 IPP-U and 78 MP pulses occurring in 3 and 10 flashes, respectively, measured at Wels at 79 km from the Gaisberg Tower. Statistics for IPP-U, MP, and all unipolar pulses are shown in the table below each histogram. No amplitude calibration was available for the Wels measurement station; see text for more details.

in the electric-field-signature parameter distributions (especially for IPP-U and MP pulses) which have relatively large ranges (minimum - maximum) and standard deviations, as seen in Figs. 7–10.

5. Summary

We examined the characteristics of electric field signatures occurring during the IS of 58 upward flashes measured simultaneously at near (170 m) and far (79 and 109 km) distances from the Gaisberg Tower. Of the 340 field signatures measured at the near station, 68 (20%) were for IPP pulses, and 272 (80%) were for MP pulses. Of the 68 IPP-pulse field signatures, 40 (59%) were of the IPP-B type and 28 (41%) were of the

IPP-U type. For the near-field signatures of IPP-B pulses, the median electric field background-to-peak risetime, 10–90% risetime, FWHM, and background-to-peak field change, were $1.0~\mu s$, $0.69~\mu s$, $0.43~\mu s$, and 0.37~kV/m, respectively. The electric field signatures of IPP-B pulses support the hypothesis that IPP-B pulses could be associated with the formation of corona/streamers preceding the development of short leader segments at the time of upward leader inception. For near-field signatures of IPP-U and MP pulses taken together, the median electric field background-to-peak risetime, 10–90% risetime, FWHM, and background-to-peak electrostatic field change, were $314~\mu s$, $156~\mu s$, $95~\mu s$, and 1.6~kV/m, respectively. For 83~(10~IPP-U~and~73~MP) pulses a radiation field peak was observed in the near electric field signature. The

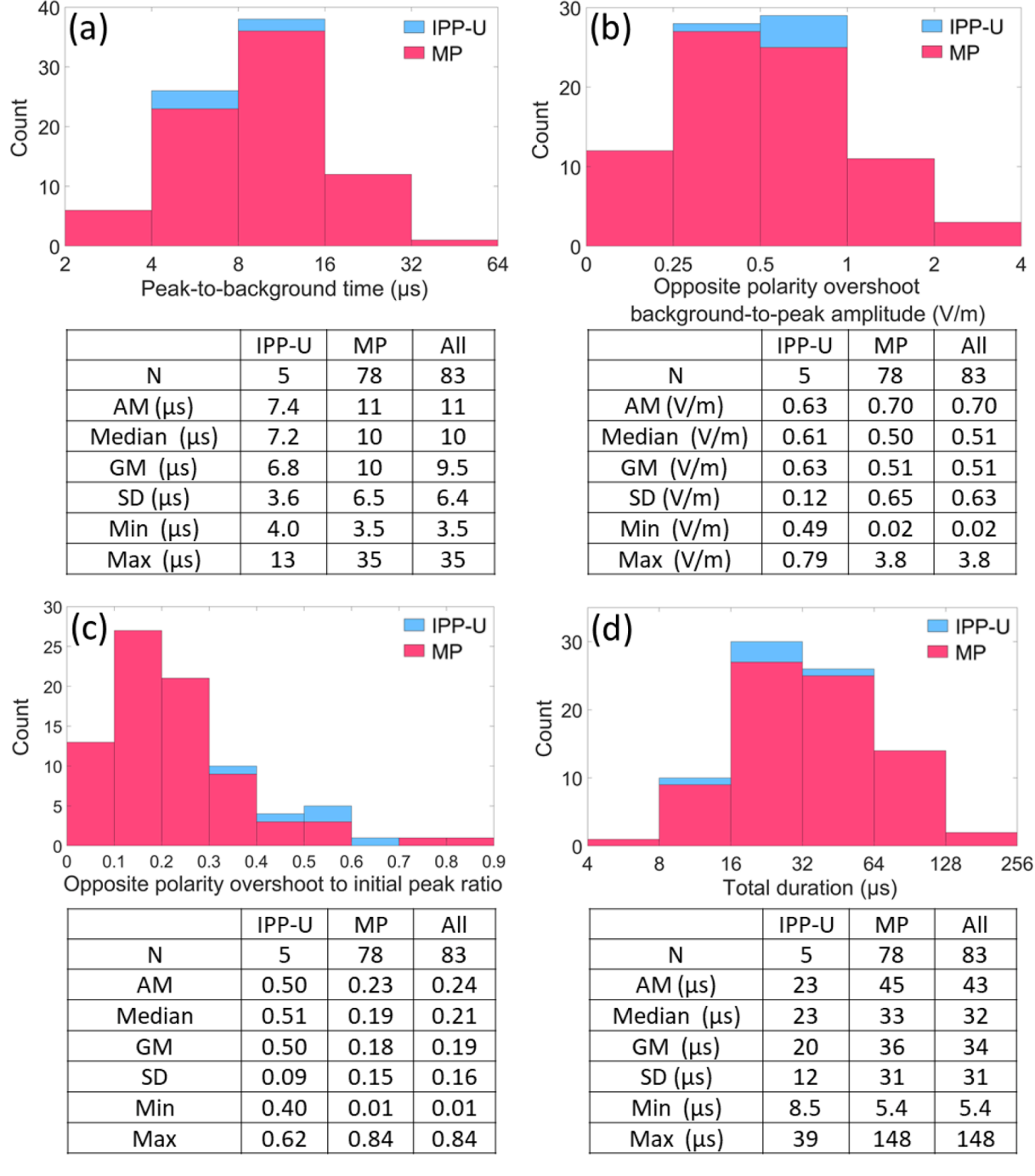


Fig. 10. Histogram of (a) peak-to-background time, (b) opposite polarity overshoot background-to-peak amplitude, (c) ratio of opposite polarity overshoot to initial peak, and (d) total duration for electric field signatures of 5 IPP-U and 78 MP pulses occurring in occurring in 3 and 10 flashes, respectively, measured at Wels at 79 km from the Gaisberg Tower. Statistics for IPP-U, MP, and all unipolar pulses are shown in the table below each histogram. Note that the horizontal axis is linear only in (c). No amplitude calibration was available for the Wels measurement station; see text for more details

median electric field background-to-peak risetime, 10–90% risetime, and background-to-peak radiation field change were $0.71~\mu s$, $0.35~\mu s$, and 1.7~kV/m, respectively. For 83 pulses recorded at the far station (Wels at 79 km), the median electric field background-to-peak risetime, 10–90% risetime, FWHM, and background-to-peak field change were $2.5~\mu s$, $1.4~\mu s$, $3.1~\mu s$, and 2.5~V/m, respectively. The median peak-to-background time, opposite polarity overshoot background-to-peak amplitude, ratio of opposite polarity overshoot to initial peak, and total duration were $10~\mu s$, 0.51~V/m, 0.21, and $32~\mu s$, respectively. There was modest correlation between the background-to-peak current and near and far electric radiation field changes as well as between near

radiation field changes and far radiation field changes of IS pulses.

CRediT authorship contribution statement

Naomi Watanabe: Methodology, Formal analysis, Writing – original draft, Visualization. Amitabh Nag: Conceptualization, Methodology, Writing – original draft, Visualization, Supervision, Funding acquisition. Gerhard Diendorfer: Writing – review & editing, Data curation, Funding acquisition. Hannes Pichler: Writing – review & editing, Data curation. Wolfgang Schulz: Writing – review & editing, Data curation. Hamid K. Rassoul: Writing – review & editing, Supervision, Funding

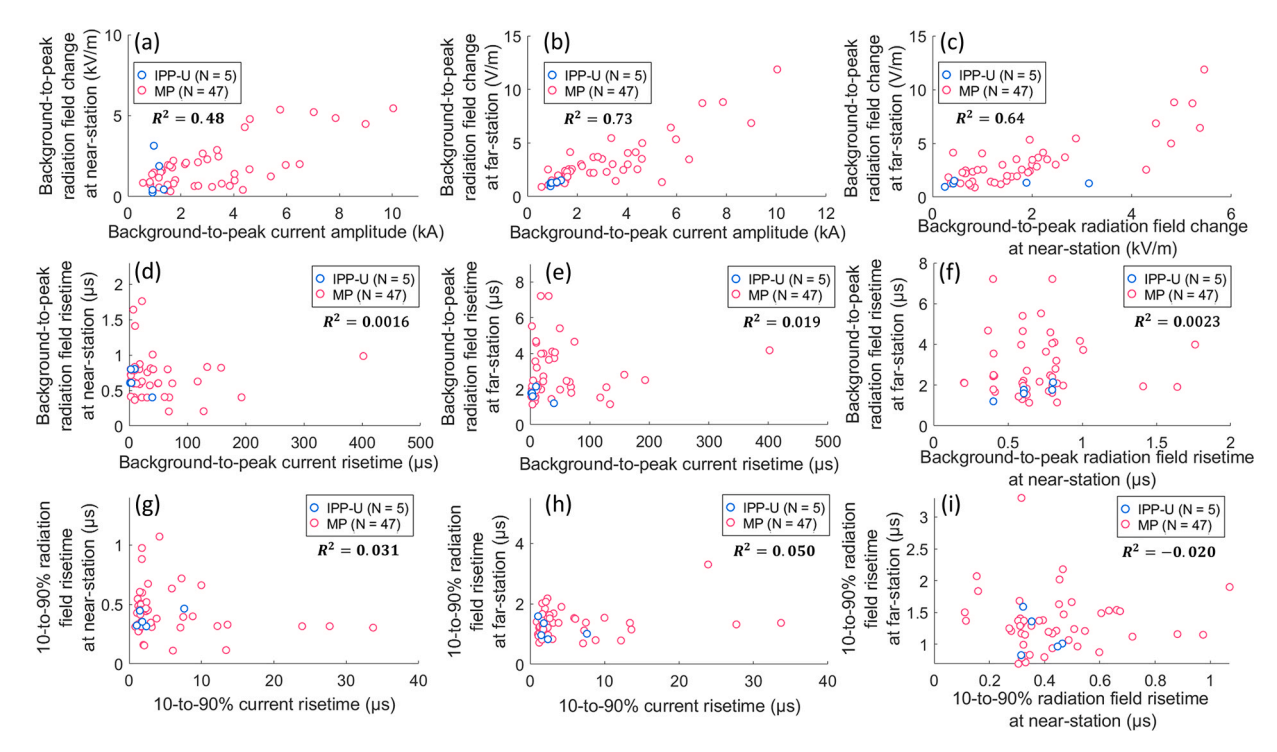


Fig. 11. Scatter plots for 52 IS pulses of background-to-peak (a) radiation field change at the near-station versus current amplitude, (b) radiation field change at far-station versus current amplitude, (c) radiation field change at far-station versus radiation field change at near-station, (d) radiation field risetime at near-station versus current risetime, (e) radiation field risetime at far-station versus current risetime, and (f) radiation field risetime at far-station versus radiation field risetime at near-station. Scatter plots for 52 IS pulses of 10–90% (g) radiation field risetime at near-station versus current risetime, (h) radiation field risetime at far-station versus current risetime, and (i) radiation field risetime at far-station versus radiation field risetime at near-station. Blue and pink color-coding indicate IPP-U and MP pulses, respectively.

acquisition.

Declaration of Competing Interest

The authors declare that they have no known competing financial interests or personal relationships that could have appeared to influence the work reported in this paper.

Data Availability

Data will be made available on request.

Acknowledgements

This study was supported in part by funding from U.S. IARPA grant 2019–19022700011, the U.S. National Science Foundation Award 1934066, and Austrian Power Grid (APG) contract 4500294593/2016. Data from the Gaisberg Tower used in this study can be obtained by contacting W. Schulz (w.schulz@ove.at).

References

- M. Azadifar, F. Rachidi, M. Rubinstein, V.A. Rakov, M. Paolone, Fast initial continuous current pulses vs return stroke pulses in tower-initiated lightning, J. Geophys. Res. Atmos. 121 (2016) 6425–6434, https://doi.org/10.1002/ 2016JD024900.
- [2] J. Hanke, Calibration of the Recording of Far Fields Radiated by Lightning Strikes to the Gaisberg Tower, Technical University Vienna, 2014.
- [3] L. He, M. Azadifar, F. Rachidi, M. Rubinstein, An analysis of current and electric field pulses associated with upward negative lightning flashes initiated from the Santis Tower, J. Geophys. Res. Atmos. 123 (2018) 4045–4059, https://doi.org/ 10.1029/2018JD028295.

- [4] H. Kohlman, W. Schulz, H. Pichler, Computation of integrator time constants for electric fiend measurements, Electric Power Syst. Res. 153 (2017) 38–45, https://doi.org/10.1016/j.epsr.2016.07.014.
- [5] A. Nag, V.A. Rakov, Positive lightning: an overview, new observations and inferences, J. Geophys. Res. 117 (2012) D08109, https://doi.org/10.1029/ 2012JD017545.
- [6] A. Nag, V.A. Rakov, J.A. Cramer, Remote measurements of currents in cloud lightning discharges, IEEE Trans. Electromagn. Compat. 53 (2) (2011), https://doi. org/10.1109/TEMC.2010.2073470. May.
- [7] H. Pichler, G. Diendorfer, M. Mair, Some parameters of correlated current and radiated field pulses from lightning to the Gaisberg Tower, IEEJ Trans. Electr. Electron. Eng. 5 (2010) 8–13, https://doi.org/10.1002/tee.20486.
- [8] M. Rubinstein, J.-L. Beemudez, V.A. Rakov, F. Rachidi, A.M. Hussein, Compensation of the instrumentatal decay in measured lightning electric field waveforms, IEEE Trans. EMC 54 (3) (2012) 685–688, https://doi.org/10.1109/ TEMC.2012.2198482.
- [9] N. Watanabe, A. Nag, G. Diendorfer, H. Pichler, W. Schulz, H.K. Rassoul, Characterization of the initial stage in upward lightning at the Gaisberg tower: 1. Current pulses, Electric Power Syst. Res. (2022) this issue.
- [10] P. Laroche, A. Eybert-Berard, L. Barret, J.P. Berlandis, Observations of preliminary discharges initiating flashes triggered by the rocket and wire technique. In Proc. 8th International Conference on Atmospheric Electricity, Uppsala, Sweden, 1988, pp. 327–333.
- [11] P. Lalande, A. Bondiou-Clergerie, P. Laroche, A. Eybert-Berard, J.P. Berlandis, B. Bador, A. Bonamy, M.A. Uman, V.A. Rakov, Leader properties determined with triggered lightning techniques, J. Geophys. Res. 103 (D12) 14 (1998) 109–115, https://doi.org/10.1029/97JD02492.
- [12] J.C. Willett, D.A. Davis, P. Laroche, An experimental study of positive leaders initiating rocket-triggered lightning, Atmos. Res. 51 (1999) 189–219, https://doi. org/10.1016/S0169-8095(99)00008-3.
- [13] H. Zhou, V.A. Rakov, G. Diendorfer, R. Thottappillil, H. Pichler, M. Mair, A study of different modes of charge transfer to ground in upward lightning, J. Atmos. Solar-Terrestrial Phys. 125-126 (2015) 38–49, https://doi.org/10.1016/j. iastb.2015.02.008.
- [14] H. Zhou, G. Diendorfer, R. Thottappillil, H. Pichler, M. Mair, Mixed mode of charge transfer to ground for initial continuous current pulses in upward lightning, in: Proceeding of the 7th Asia-Pacific International Conference on Lightning, Chengdu, China, 2011, https://doi.org/10.1109/apl.2011.6110212.